Identification and Characterization of Membrane Androgen Receptors in the ZIP9 Zinc Transporter Subfamily: II. Role of Human ZIP9 in Testosterone-Induced Prostate and Breast Cancer Cell Apoptosis

Peter Thomas, Yefei Pang, Jing Dong, and A. Håkan Berg

Marine Science Institute (P.T., Y.P., J.D., A.H.B.), The University of Texas at Austin, Port Aransas, Texas 78373; and Department of Science and Technology (A.H.B.), Örebro University, Örebro, Sweden SE-70182

Recently, we discovered a cDNA in teleost ovarian follicle cells belonging to the zinc transporter ZIP9 subfamily (SLC39A9) encoding a protein with characteristics of a membrane androgen receptor (mAR). Here, we demonstrate that human ZIP9 expressed in MDA-MB-468 breast cancer cells and stably overexpressed in human prostate cancer PC-3 cells (PC-3-ZIP9) also displays the ligand binding and signaling characteristics of a specific, high-affinity mAR. Testosterone treatment of MDA-MB-468 and PC-3-ZIP9 cells caused activation of G proteins and second messenger pathways as well as increases in intracellular free zinc concentrations that were accompanied by induction of apoptosis. [1,2,6,7-^{3}H]-testosterone binding and these responses were abrogated in MDA-MB-468 cells after ZIP9 small interfering RNA (siRNA) treatment and absent in PC-3 cells transfected with empty vector, confirming that ZIP9 functions as an mAR. Testosterone treatment caused up-regulation of proapoptotic genes Bax (Bcl-2-associated X protein), p53 (tumor protein p53), and JNK (c-Jun N-terminal kinases) in both cell lines and increased expression of Bax, Caspase 3, and cytochrome C proteins. Treatment with a zinc chelator or a MAPK inhibitor blocked testosterone-induced increases in Bax, p53, and JNK mRNA expression. The results suggest that both androgen signaling and zinc transporter functions of ZIP9 mediate testosterone promotion of apoptosis. ZIP9 is widely expressed in human tissues and up-regulated in malignant breast and prostate tissues, suggesting that it is a potential therapeutic target for treating breast and prostate cancers. These results provide the first evidence for a mechanism mediated by a single protein through which steroid and zinc signaling pathways interact to regulate physiological functions in mammalian cells. **(*Endocrinology* 155: 4250–4265, 2014)**

The physiological importance of rapid, cell surface-initiated steroid actions in regulating cellular functions through activation of intracellular signaling pathways has become widely acknowledged with the publication of numerous studies on these nonclassical steroid actions in a broad range of vertebrate cells and tissues (1–3). Both nuclear steroid receptors in extranuclear locations and novel 7-transmembrane receptors unrelated to nuclear steroid receptors have been implicated as intermediaries in these rapid, pregenomic steroid actions (4–9). Within the last decade, novel membrane receptors have been identified for progesterone, membrane progesterone receptors (mPRs), and for estrogens, G protein-coupled estrogen receptor-1 (GPER, formally known as G protein-coupled receptor 30, GPR30) (10–13), which has prompted intensive research on their functions in health and disease. Al-

ISSN Print 0013-7227 ISSN Online 1945-7170
Printed in U.S.A.

Received March 6, 2014. Accepted July 3, 2014.
First Published Online July 11, 2014

For News & Views see page 4120; for related article see page 4237

Abbreviations: Bax, Bcl-2-associated X protein; B_{max}, maximum binding capacity; GTPγS, guanosine 5′-O-[gamma-thio] triphosphate; $G_{\alpha i}$, G protein α inhibitory; $G_{\alpha s}$, G protein α stimulatory; [^{3}H]-T, [1,2,6,7-^{3}H]-testosterone; JNK, c-Jun N-terminal kinases; K_d, dissociation constant; mAR, membrane androgen receptor; nAR, nuclear AR; p53, tumor protein p53; PD98059, 2-(2-Amino-3-methoxyphenyl)-4H-1-benzopyran-4-one; q-PCR, quantitative real-time PCR; siRNA, small interfering RNA; SLC, solvent-linked carrier protein 30; TPEN, N,N,N′,N′-Tetrakis(2-pyridylmethyl)ethylenediamine; TUNEL,Terminal deoxynucleotidyl transferase dUTP nick end labeling; ZIP, Zrt- and Irt-like proteins (SLC39A0).

though androgens have also been shown to exert nonclassical actions in a variety of cell types (2, 14–20), the membrane androgen receptors (mARs) mediating these actions have not been identified. The finding that nuclear AR (nAR) agonists, such as R1881 (methyltrienolone) and mibolerone, and antiandrogens, such as flutamide and cyproterone acetate, do not bind to mARs or influence nonclassical androgen actions in many cells (9, 16, 18, 21–23) suggests the existence of novel androgen receptors unrelated to the nAR. The identification of nonclassical androgen actions in cells and animal models that do not express the nAR (9, 24, 25) further suggests the existence of a novel mAR. However, failure to identify the mAR has hindered progress in determining the mechanisms of androgen action and in developing therapies that target the mAR to treat human diseases. For example, although an unidentified mAR been implicated in mediating apoptotic actions of androgens in prostate cancer cells and tumor regression when the cells are transplanted into mice (24), selective agonists that do not activate nuclear receptors, like those developed for mPRs and GPER (26, 27), have not been developed for the mAR.

Significant progress has also recently been made in deciphering the critical roles of another major regulator of essential structural and cellular functions in vertebrates, the trace element zinc (28, 29). Zinc regulates the expression of numerous genes (30) and is a cofactor for over 50 enzymes regulating metabolism (31). More than 3% of human genes encode for proteins with zinc-binding motifs called zinc fingers that includes proteins involved in immune function, proliferation, differentiation, signal transduction, cell adhesion, and apoptosis (32–34). Disruptions of zinc homeostasis are associated with a variety of diseases, including diabetes, cancer, and immune and connective tissue disorders (30, 32, 34–37). Because zinc status is a crucial factor influencing normal cell physiology, a complex multifaceted zinc transporter system tightly regulates intracellular zinc levels within narrow limits (28, 30, 35, 37, 38). The 10 members of the human ZnT (zinc transporter, vertebrate cation diffusion facilitator family proteins [SLC30A, solute-linked carrier 30]) zinc transporter family regulate zinc export from cells, whereas the 14 members of the human ZIP (Zrt-and Irt-like proteins [SLC39A]) zinc transporter family increase intracellular free zinc levels by facilitating zinc influx from the extracellular fluid or its release from intracellular stores (28, 37). However, despite their importance in maintaining zinc homeostasis and in mediating zinc-transduction pathways controlling vital cellular functions, hormonal regulation of ZnT and ZIP zinc transporter functions has not been investigated extensively and remains poorly understood.

Recently, we identified a cDNA encoding a novel mAR in Atlantic croaker ovaries that has high sequence identity with members of the vertebrate ZIP9 (SLC39A9) subfamily. The croaker ZIP9 protein has all the characteristics of a mAR and mediates androgen-induced apoptosis of ovarian follicle cells as well as increases in intracellular free zinc concentrations (64). This discovery provides an initial indication that zinc transporter proteins can also function as steroid hormone receptors and indicates a plausible mechanism by which steroid hormones can regulate physiological functions through regulating zinc homeostasis. Thus, these findings suggest that there are direct interactions between nonclassical steroid hormone actions and zinc-dependent signaling and functions. However, structural modeling predicts that croaker ZIP9 has 7 transmembrane domains with an intracellular C terminus, whereas other ZIP9s in most fish and in mammalian species are predicted to have 8 transmembrane domains with extracellular C termini (34, 37, 38). Little information is currently available on tetrapod ZIP9s (38, 39), but recent evidence indicates that ZIP9 is present on the *trans*-Golgi apparatus (38), a location inconsistent with its function as a mAR. Therefore, the broad applicability of the results obtained with croaker ZIP9 remains unclear.

In the present study, we tested the hypothesis that human ZIP9 functions as a mAR and mediates apoptotic actions of androgens. Testosterone acts on the cell surface of human prostate and breast cancer cells to induce apoptosis through an unidentified mAR (24, 40). ZIP9 is a plausible candidate for the mAR mediating testosterone's apoptotic actions in these cancer cells. Therefore, mAR functions of human ZIP9 were investigated in triple-negative human breast cancer MDA-MB-468 cells, which express moderate levels of ZIP9, and in nAR-negative PC-3 human prostate cancer cells with lower levels of ZIP9, in which ZIP9 was overexpressed by stable transfection. Testosterone activation of intracellular signaling, apoptosis, and apoptotic pathways was investigated in these cell lines. In addition, ZIP9 mRNA expression in human breast and prostate cancer biopsy samples was compared with that in normal tissue controls. The results show human ZIP9 functions as a mAR and zinc transporter in both breast cancer and prostate cancer cell lines and mediates testosterone-induced apoptosis through MAPK- and zinc-dependent pathways in these cells.

Materials and Methods

Chemicals

[1,2,6,7-^{3}H]-testosterone ([^{3}H]-T) (83.4 Ci/mmol) and [^{35}S]-GTPγS (guanosine 5′-O-[gamma-thio] triphosphate, 1250 Ci/

mmol) were purchased from PerkinElmer. All other chemical reagents were purchased from Sigma-Aldrich or Steraloids unless otherwise stated. Antibodies are listed in Supplemental Table 1.

Expression of recombinant ZIP9 in human prostate and breast cancer cell lines

Full-length cDNA clones encoding human SLC39A9/ZIP9 (NM_018375; Origene) were subcloned into pCMV6-Neo mammalian expression vectors (Origene), and constructs or empty vector were transfected into human PC-3 cells and MDA-MB-231 cells (American Type Culture Collection) with Lipofectamine 2000 (Invitrogen) following the manufacturer's instructions. Transfected cells were selected with 500-μg/mL geneticin (G418; Invitrogen) and cultured in DMEM/Ham's nutrient medium containing 10% charcoal-stripped fetal calf serum. Transfected cells were used in experiments after 2–3 passages when ZIP9 expression was maximal. MDA-MB-468 and LNCaP cells, not transfected with ZIP9 or empty vector, were transiently transfected with ZIP9 siRNA (small interfering RNA) and nontarget siRNA (100nM, SmartPool; Dharmacon) using Lipofectamine 2000 twice at 0 and 16 hours, and experiments were performed 2 days later.

RT-PCR and quantitative real-time PCR (q-PCR)

Reverse transcription of extracted total RNA was performed using SuperScript III reverse transcriptase (Invitrogen) and oligo (dT) primers. PCR was conducted using GoTaq Green Master Mix (Promega) as described previously (41) using the following gene-specific primers for ZIP9 (sense, 5′-CTCTTGGAACCACCACACCT-3′ and antisense, 5′-CCCAAAACAGTCACCAGCTT-3′), Bax (Bcl-2-associated X protein) (sense, 5′-TTTGCTTCAGGGTTTCATCC-3′ and antisense, 5′- CAGTTGAAGTTGCCGTCAGA-3′), JNK (c-Jun N-terminal kinases) (sense, 5′-TTGGAACACCATGTCCTGAA-3′ and antisense, 5′-ATGTACGGGTGTTGGAGAGC-3′), and p53 (tumor protein p53) (sense, 5′-GTTCCGAGAGCTGAATGAGG-3′ and antisense, 5′-TCTGAGTCAGGCCCTTCTGT-3′). A housekeeping gene, β-actin (sense, 5′-AAGAGAGGCATCCTCACCCT-3′ and antisense, 5′-TACATGGCTGGGGTGTTGAA-3′), was used as a loading control. q-PCR assays were performed using an Eppendorf RealPlex Mastercycler (Eppendorf), in a 25-μL one-step Brilliant II SYBR Green q-PCR Master Mix (Agilent) containing 100nM of the same gene-specific primers (41).

Western blot analysis and immunocytochemistry

Subcellular protein fractions were resolved on 10% SDS-PAGE gels, transferred to nitrocellulose membranes, blocked with 5% nonfat milk, and incubated overnight with a custom polyclonal antibody (1:2000) raised in rabbits against a synthetic 14-mer peptide (AEKSVVHEHEHSDC) derived from the first extracellular loop from the N-terminal end of human ZIP9 protein (GenScript). Membranes were then incubated for 1 hour with the second antibody (1:5000 horseradish peroxidase conjugated to goat antirabbit) and detected with SuperSignal (Pierce). Immunocytochemistry was performed on cells grown on coverslips, fixed in 2% paraformaldehyde for 15 minutes, blocked for 1 hour with 2% BSA in PBS, and followed by an overnight incubation in primary antibody (1:500). Cells were then incubated for 1 hour with second antibody (1:2000) goat antirabbit Alexa Fluor 488 (Molecular Probes) and mounted using ProLong Gold Antifade Reagent with DAPI (4′,6-diamidino-2-phenylindole, Molecular Probes) and visualized using a fluorescent microscope.

Preparation of plasma membranes and other subcellular fractions

Cells were homogenized with a sonicator in buffer at 4°C containing 1% protease inhibitor cocktail (Pierce). Subcellular fractions were isolated by differential centrifugation as described previously (42, 43).

AR binding assays

Saturation analysis of [^{3}H]-T binding (range, 0.25nM to 25nM) alone (total binding), or with 100-fold excess nonradiolabeled testosterone (nonspecific binding), to plasma membranes of MDA-MB-468 and PC-3-ZIP9 cells after 30 minutes of incubation at 4°C was determined by filtration assay as described previously (18). Competitive binding assays were conducted in triplicate with steroid competitors (range, 10^{-5}M to 10^{-10}M), incubated with 4nM [^{3}H]-T, and the results expressed as a percentage of maximum specific testosterone binding.

Human breast and prostate cancer tissues

Human tissue RNA samples obtained from healthy adults were purchased from Biochain. Deidentified paired normal and malignant human breast and prostate tissue samples were obtained from the National Cancer Institute Human Tissue Network. Samples were handled in accordance with National Institutes of Health guidelines approved by The University of Texas Office of Research Support and Compliance. Frozen samples were stored at −80°C until analyzed by q-PCR. Paraffin-embedded tissues were sectioned, deparaffinized in xylene, rehydrated in a series of ethanol solutions, and washed with PBS. Tissue sections were blocked with 2% BSA in PBS and incubated with ZIP9 (1:500) or nAR (1:500) antibodies overnight followed by 1-hour incubation with goat antirabbit Alexa Flour 488 or Texas Red secondary antibody at room temperature. Presence of fluorescent-labeled ZIP9 protein in tissue sections was examined using a Nikon fluorescent microscope and imaging system.

G protein activation and immunoprecipitation

G protein activation was assessed by measuring [^{35}S]-GTPγS binding to cell plasma membranes after incubation with 100nM androgens or vehicle for 45 minutes at 28°C as described previously (12, 17). Membrane-bound [^{35}S]-GTPγS-labeled G protein α-subunits activated by testosterone were identified by immunoprecipitation with G protein α-inhibitory ($G_{\alpha i}$) and G protein α-stimulatory ($G_{\alpha s}$) antibodies (1:100; Santa Cruz Biotechnology, Inc) (12, 17).

Apoptosis and Caspase 3 assays

Cells were serum starved for 48 hours and then incubated in serum-free media containing steroids for 36–48 hours. Cells were fixed with 4% paraformaldehyde, followed by 5 minutes staining with 1 μg/μL Hoechst 33342. Cells were then washed and observed under a fluorescent microscope. Apoptotic nuclei were counted and expressed as percent apoptotic cells. Apoptotic cells were also detected by TUNEL (Terminal deoxynucleotidyl transferase dUTP nick end labeling) assay using an ApoAlert

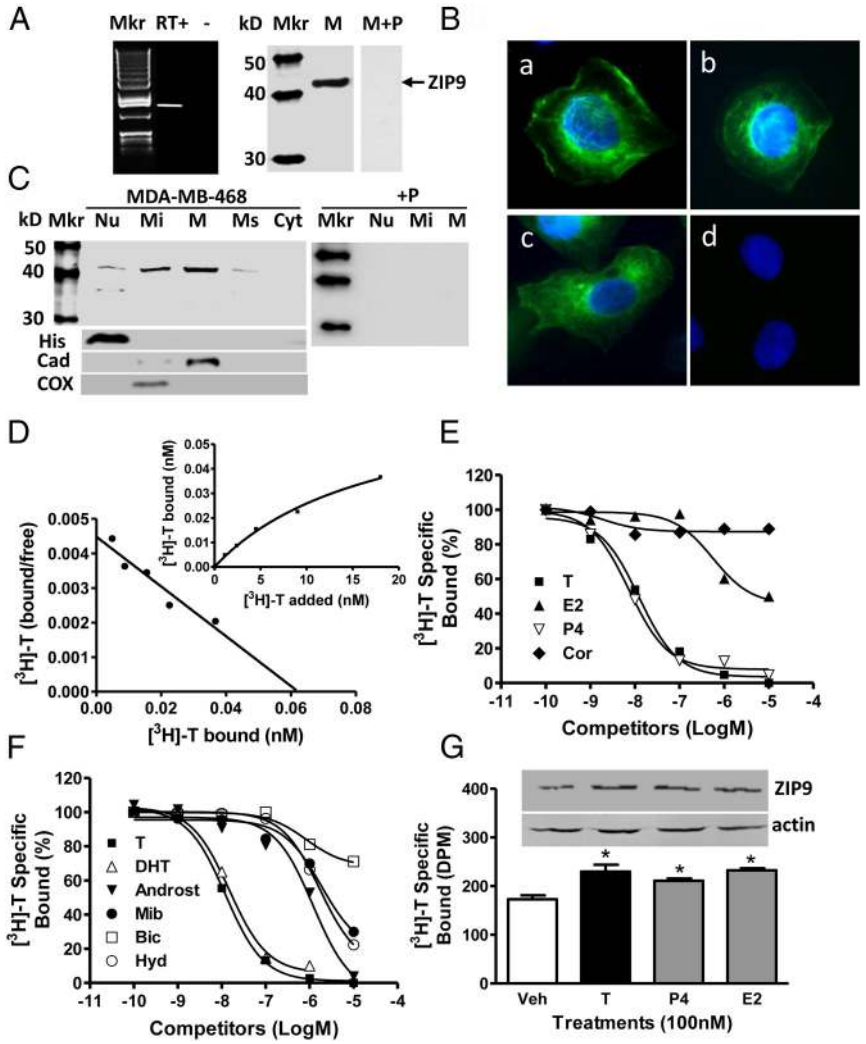

Figure 1. Membrane androgen binding and expression of ZIP9 in nAR-negative MDA-MB-468 human breast cancer cells. A–C, Expression of ZIP9 mRNA (left) and ZIP9 protein on plasma membranes (6 μg/lane) (right) (A) and ZIP9 protein localization in cells by immunocytochemical analysis (B, a–c; peptide block, d) and in subcellular fractions by Western blot analysis (10 μg/lane) (C). Mkr, 100-bp ladder or molecular weight marker; +P, peptide block; actin, actin loading control; Nu, nuclear fraction; Mi, mitochondrial faction; M, plasma membrane fraction; Ms, microsomal fraction; Cyt, cytoplasmic fraction; His, histone nuclear marker; Cad, cadherin plasma membrane marker; COX, cyclooxygenase mitochondrial marker. The purity of subcellular fractions was confirmed using antibodies to these specific marker proteins. D, Representative saturation analysis and Scatchard plot of specific [^{3}H]-T binding to plasma membranes. E and F, Representative competition curves of steroid binding to plasma membranes expressed as a percentage of maximum [^{3}H]-T binding. T, testosterone; DHT, 5α-dihydrotestosterone; Androst, androstenedione; Cor, cortisol; E2, estradiol-17β; P4, progesterone; mib, mibolerone; Bic, bicalutamide; Hyd, hydroxyflutamide. G, Effects of overnight treatment of MDA-MB-468 cells with 100nM T, P4, and E2 on plasma membrane expression of ZIP9 protein (top) and specific [^{3}H]-T plasma membrane binding (bottom). *, $P < .05$ compared with vehicle (Veh) control, n = 6.

DNA fragmentation Assay kit (Clontech) following the manufacturer's instructions. Caspase 3 activity was measured by fluorescence assay using an ApoAlert kit (Clontech).

Intracellular zinc measurement

Changes in intracellular zinc levels in cells in response to steroid treatments (20 min) were determined using a specific fluorescent probe for zinc, Zinquin ethyl ester (15μM; Molecular Probes), and fluorescence ($_{exc}$ 365 nm, $_{em}$ 420 nm) was measured under a fluorescent microscope (44), or with a 96-well fluorescence plate reader.

cAMP and MAPK assays

cAMP concentrations were measured in cell lysates after incubation with androgens for 20 minutes with an enzyme immunoassay kit (Cayman Chemical) following the manufacturer's instructions. Phosphorylation of ERK was measured by Western blot analysis as described previously (26). Cells were cultured overnight in serum-free medium to reduce background activity before conducting experiments.

Statistical analysis

All data are reported as mean values ± SEM of at least 3 measurements in a single experiment. All experiments were repeated at least 3 times, and similar results were obtained on each occasion. Significant differences between paired treatment groups were analyzed by Student's paired *t* test (GraphPad Prism Software).

Results

ZIP9 localization in MDA-MB-468 cells

RT-PCR produced a band of the predicted size for ZIP9 in triple-negative MB-MDA-468 breast cancer cells, which was absent in RT− controls (Figure 1A, left). Western blot analysis of MDA-MB-468 plasma membranes with human ZIP9 antibody showed a single band, size approximately 43-kDa, which was absent after preincubation of the antiserum with peptide antigen (M+P, Figure 1A, right). Immunocytochemical analysis showed ZIP9 protein is distributed in the perinuclear region and on the plasma membrane of MDA-MB-468 cells (Figure 1B, a–c). The immunostaining was blocked after preincubation of the antibody with peptide antigen, confirming the specificity of the immunoreaction (Figure 1B, d). Western blot analysis of subcellular fractions containing the same protein concentrations showed strong protein bands, approximately 43-kDa, in plasma membrane and mitochondrial

fractions, which were blocked by preincubation with peptide antigen, and lower expression in nuclear and microsomal fractions (Figure 1C). A weaker secondary immunoreactive band (~37 kDa) was also detected in the nuclear fraction.

[^{3}H]-T binding characteristics of MDA-MB-468 cells

Saturation and Scatchard plot analyses of [^{3}H]-T binding showed the presence of a high-affinity (dissociation constant, K_d, 17.9 ± 3.4nM), limited capacity (maximum binding capacity, B_{max}, 4.1 ± 0.5nM/mg membrane protein), single binding site on plasma membranes of MDA-MB-468 cells (Figure 1D). Competitive binding studies showed that progesterone was as effective as testosterone in displacing [^{3}H]-T binding from plasma membranes, whereas cortisol and estradiol-17β were ineffective competitors (Figure 1E). Of the androgens tested, dihydrotestosterone displayed a binding affinity almost identical to that of testosterone, whereas androstenedione, the nAR agonist mibolerone, and the nAR antiandrogen hydroxyflutamide had affinities less than 1% that of testosterone, and the nAR antiandrogen bicalutamide (Casodex) had negligible affinity for the receptor (Figure 1F). Treatment of MDA-MB-468 cells overnight with 100nM testosterone, progesterone and estradiol-17β increased ZIP9 protein concentrations on plasma membranes, which was associated with parallel increases in specific [^{3}H]-T binding (Figure 1G).

Testosterone induction of signaling and apoptosis through ZIP9 in MDA-MB-468 cells

Treatment with testosterone (100nM) significantly increased specific [^{35}S]-GTPγS membrane binding which was not observed with mibolerone, suggesting that G proteins are activated by a novel mAR (Figure 2A). Immunoprecipitation of membrane-bound [^{35}S]-GTPγS with specific G protein α-subunit antibodies showed that most of the elevated [^{35}S]-GTPγS after testosterone treatment was bound to an inhibitory G protein $G_{\alpha i}$-subunit and practically none to the $G_{\alpha s}$-subunit (Figure 2B). Testosterone (20nM and 100nM) treatment for 15 minutes increased ERK phosphorylation, whereas 100nM mibolerone was ineffective (Figure 2C). Treatment with 20nM, 50nM, and 100nM testosterone and 100nM testosterone conjugated to bovine serum albumen (testosterone-BSA) caused significant increases in intracellular free zinc concentrations, whereas 100nM mibolerone, dihydrotestosterone, progesterone, estradiol-17β, and cortisol did not alter zinc levels (Figure 2, D and E). Treatment of serum-starved cells with 20nM and 100nM testosterone for 48 hours caused a concentration-dependent increase in percent apoptotic nuclei, which was mimicked by testosterone-BSA (100nM), but not by the other steroids tested (Figure 2F). The percent apoptotic nuclei was also significantly increased after treatment with 20nM testosterone and testosterone-BSA assessed by TUNEL assay (Figure 2G). Caspase 3 activity was significantly increased within 5 hours of treatment with 20nM testosterone but not with mibolerone (Figure 2H). Transient transfection of ZIP9 siRNA decreased ZIP9 expression and specific [^{3}H]-T binding to MDA-MB-468 cell membranes (Figure 2I), which was accompanied by a complete loss of the intracellular free zinc response to testosterone treatment (Figure 2J) as well as testosterone-induced apoptosis (Figure 2K).

ZIP9 localization in ZIP9-transfected PC-3 cells

Relatively low levels of ZIP9 expression were detected in nAR-negative PC-3 prostate cancer cells transfected with vector alone (PC-3-Vec), whereas expression was increased after stable transfection of ZIP9 (PC-3-ZIP9) (Figure 3A). Immunocytochemical analysis showed ZIP9 is predominantly localized to the perinuclear region with significant expression also on the plasma membrane in PC-3-ZIP9 cells (Figure 3B). Western blot analysis of subcellular fractions (20μg protein/lane, twice that used in the Western blot in Figure 3A) showed greatest expression of the major protein band (~43-kDa) in the plasma membrane and a weaker band in mitochondrial fractions of PC-3-Vec cells, whereas a smaller lower molecular weight band (~37-kDa) was detected in the nuclear fraction (Figure 3C). ZIP9 protein expression was further increased in plasma membrane, mitochondrial, and nuclear fractions of PC-3-ZIP9 cells, and faint larger molecular weight (~43-kDa) bands in addition to stronger smaller molecular weight (~37-kDa) bands were detected in nuclear fractions (Figure 3C). The subcellular localization of ZIP9 in these cells was confirmed using specific subcellular markers (Figure 3C) and another human ZIP9 antibody (Supplemental Figure 1). Smaller (~33 kDa) bands were observed in membrane and nuclear fractions of PC-3-ZIP9 cells after deglycosylation (M+E, Figure 3C), which correspond to the predicted molecular weight of ZIP9.

[^{3}H]-T binding characteristics in PC-3-ZIP9 cells

Increased plasma membrane expression of ZIP9 in PC-3-ZIP9 cells compared with PC-3-Vec cells was associated with an approximately 2-fold increase in specific [^{3}H]-T membrane binding (Figure 3D). Saturation analysis and Scatchard plots of [^{3}H]-T binding to PC-3-ZIP9 cell membranes demonstrated high-affinity, limited-capacity, single, specific [^{3}H]-T binding sites with a K_d of 14.4 ± 2.4nM and a B_{max} of 7.4 ± 0.6nM/mg protein (Figure 3E). Competitive binding assays with PC-3-ZIP9 cell mem-

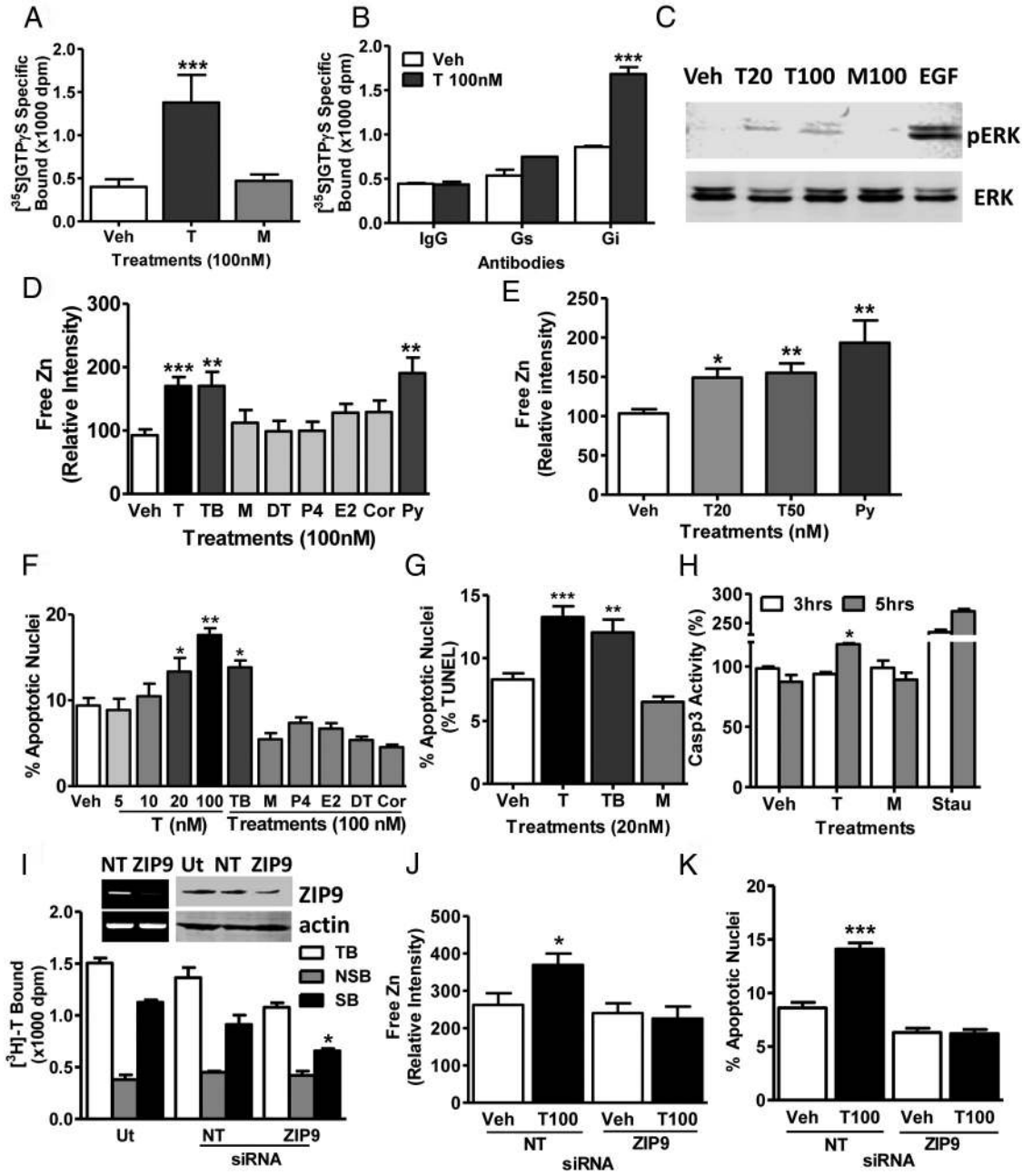

Figure 2. Effects of androgens on signal transduction pathways and apoptosis through ZIP9 in MDA-MB-468 cells. A, Effects of androgens (100nM) on [^{35}S]-GTPγS binding to plasma membranes. T, testosterone; M, mibolerone. ***, $P < .001$ compared with vehicle (Veh) control, n = 6. B, Immunoprecipitation of [^{35}S]-GTPγS bound to G protein α-subunits on plasma membranes activated by 100nM T treatment with specific G protein α-subunit antibodies or control IgG. Gs, $G_{\alpha s}$ antibody; Gi, $G_{\alpha i}$ antibody. ***, $P < .001$ compared with corresponding IgG control, n = 6. C, Representative Western blot showing the effects of 15 minutes treatments with T (20, 100nM) and M (100nM) on activation of ERK1/2. EGF, epidermal growth factor-positive control; pERK, phosphorylated ERK. D and E, Effects of T and other steroid treatments on relative intracellular free zinc levels. Py, pyrithione-positive control; TB, charcoal-stripped T bovine serum albumen conjugate; DT, dihydrotestosterone; E2, estradiol-17β; P4, progesterone; Cor, cortisol. ***, $P < .001$; **, $P < .01$ compared with Veh control. F and G, Effects of T and other steroids on % apoptotic nuclei in Hoechst (F) and TUNEL (G) assays. H, Effects of treatment with 20nM T and M for 3 and 5 hours on Caspase 3 activity. Stau, staurosporin (600nM); *, $P < .05$ compared with respective Veh control. I–K, Effects of knockdown of ZIP9 expression by transfection with siRNA (ZIP9) and nontarget siRNA controls (NT) on ZIP9 mRNA expression (I, top, left) and ZIP9 protein expression in plasma membranes (I, top, right) and [^{3}H]-T binding in a single-point assay (bottom) (I) as well as intracellular zinc concentrations (J) and apoptosis (K) in response to 100nM T. Actin, loading controls; Ut, untransfected controls; TB, total binding; NSB, nonspecific binding; SB, specific binding. ***, $P < .001$; *, $P < .05$ compared with respective NT-specific binding (G) or Veh NT controls (H), n = 6.

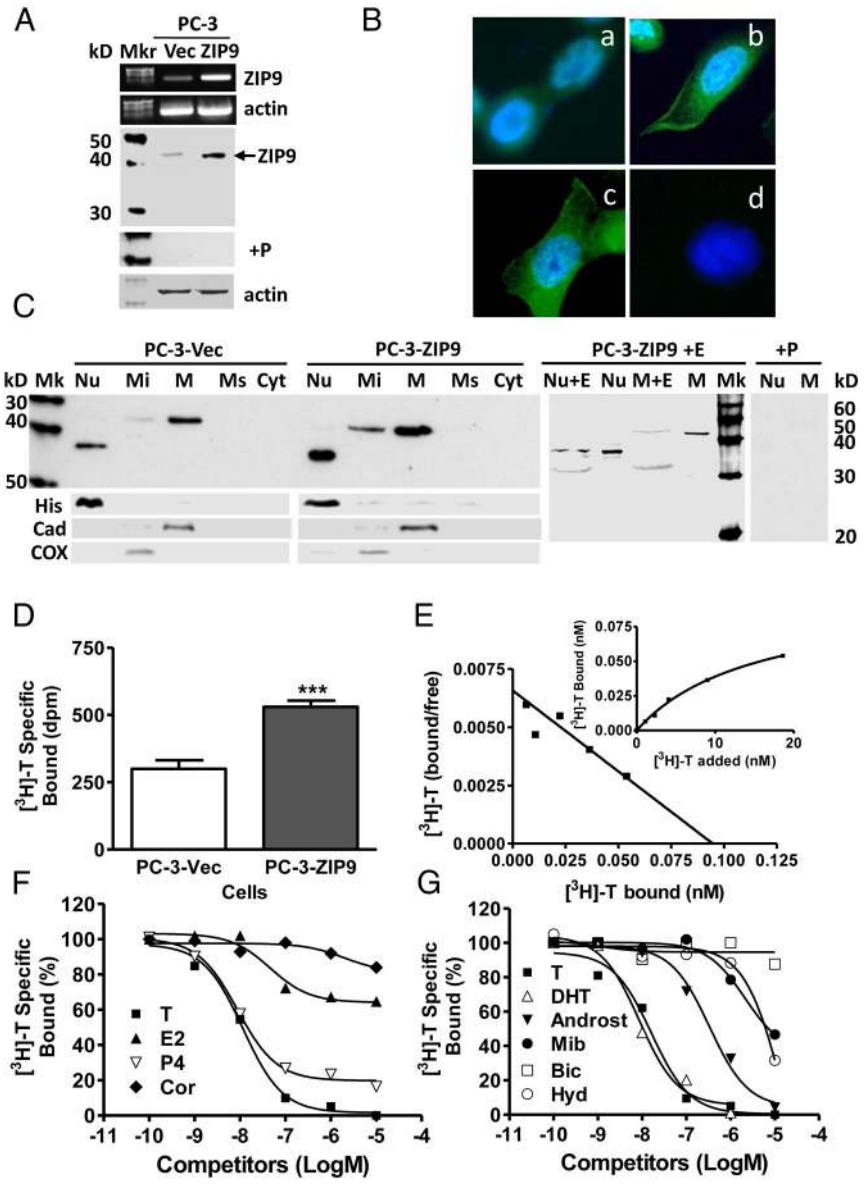

Figure 3. Membrane androgen binding and expression of ZIP9 in nAR-negative PC-3 human prostate cancer cells overexpressing ZIP9 (PC-3-ZIP9) and in cells transfected with vector alone (PC-3-Vec). A–C, Expression of ZIP9 mRNA (top) and protein on plasma membrane (bottom) (A), by immunocytochemical analysis (B), and ZIP9 protein expression in subcellular fractions by Western blot analysis (C). Protein loading (20 μg/lane) for the Western blotting in C was double that in A to detect minor immunoreactive bands. Mkr, molecular weight marker; M+E, deglycosylated plasma membranes; +P, peptide block; actin, loading control; (see Figure 1 for key to subcellular abbreviations and markers). D, Representative single-point binding assay of specific [^{3}H]-T binding to plasma membranes of PC-3-ZIP9 and PC-3-Vec cells. ***, $P < .001$ compared with PC-3-Vec cell membranes, n = 6. E, Representative saturation analysis and Scatchard plot of specific [^{3}H]-T binding to cell membranes of PC-3-ZIP9 cells. F and G, Representative competition curves of steroid binding to cell membranes of PC-3-ZIP9 cells expressed as a percentage of maximum [^{3}H]-T binding (see Figure 1 for key to steroid abbreviations).

branes showed similar steroid specificities to those observed in MDA-MB-468 cells, with dihydrotestosterone and progesterone displaying the same high relative binding affinities as testosterone, whereas androstenedione, mibolerone and hydroxyflutamide had lower affinities and bicalutamide, estradiol-17β, and cortisol were ineffective as competitors (Figure 3, F and G).

Testosterone induction of signaling and apoptosis through ZIP9 in PC-3-ZIP9 cells

Treatment with 100nM testosterone, but not with mibolerone, caused significant G protein activation in PC-3-ZIP9 cells, as shown by increased [^{35}S]-GTPγS binding to plasma membranes, whereas no G protein activation was observed in PC-3-Vec cells (Figure 4A). Immunoprecipitation of membrane-bound [^{35}S]-GTPγS on PC-3-ZIP9 cells with G protein α-subunit antibodies showed that all the increased membrane-associated [^{35}S]-GPTγS after testosterone treatment was bound to an inhibitory $G_{\alpha i}$ (Figure 4B). Consistent with these findings, testosterone and dihydrotestosterone (20nM, 100nM) caused concentration-dependent decreases in cAMP production in PC-3-ZIP9 cells compared with vehicle-treated controls, whereas these treatments were ineffective in PC-3-Vec cells (Figure 4C). Testosterone treatment (20nM) also increased intracellular free zinc levels in PC-3-ZIP9 cells but was ineffective in PC-3-Vec cells (Figure 4D). The testosterone-induced increase in free zinc was concentration-dependent over the range of 5nM to 100nM and mimicked with testosterone-BSA, which suggests that this testosterone action is initiated at the cell surface (Figure 4E). Dihydrotestosterone and mibolerone treatments (100nM) also increased zinc concentrations whereas progesterone, estradiol-17β, and cortisol were ineffective (Figure 4F). Caspase 3 activity was increased after 5 hours of treatment with 20nM testosterone, whereas mibolerone was ineffective at this concentration (Figure 4G). Treatment with 20nM testosterone and testosterone-BSA, but not mibolerone, significantly increased percent apoptotic nuclei in PC-3-ZIP9 cells but not in PC-3-Vec

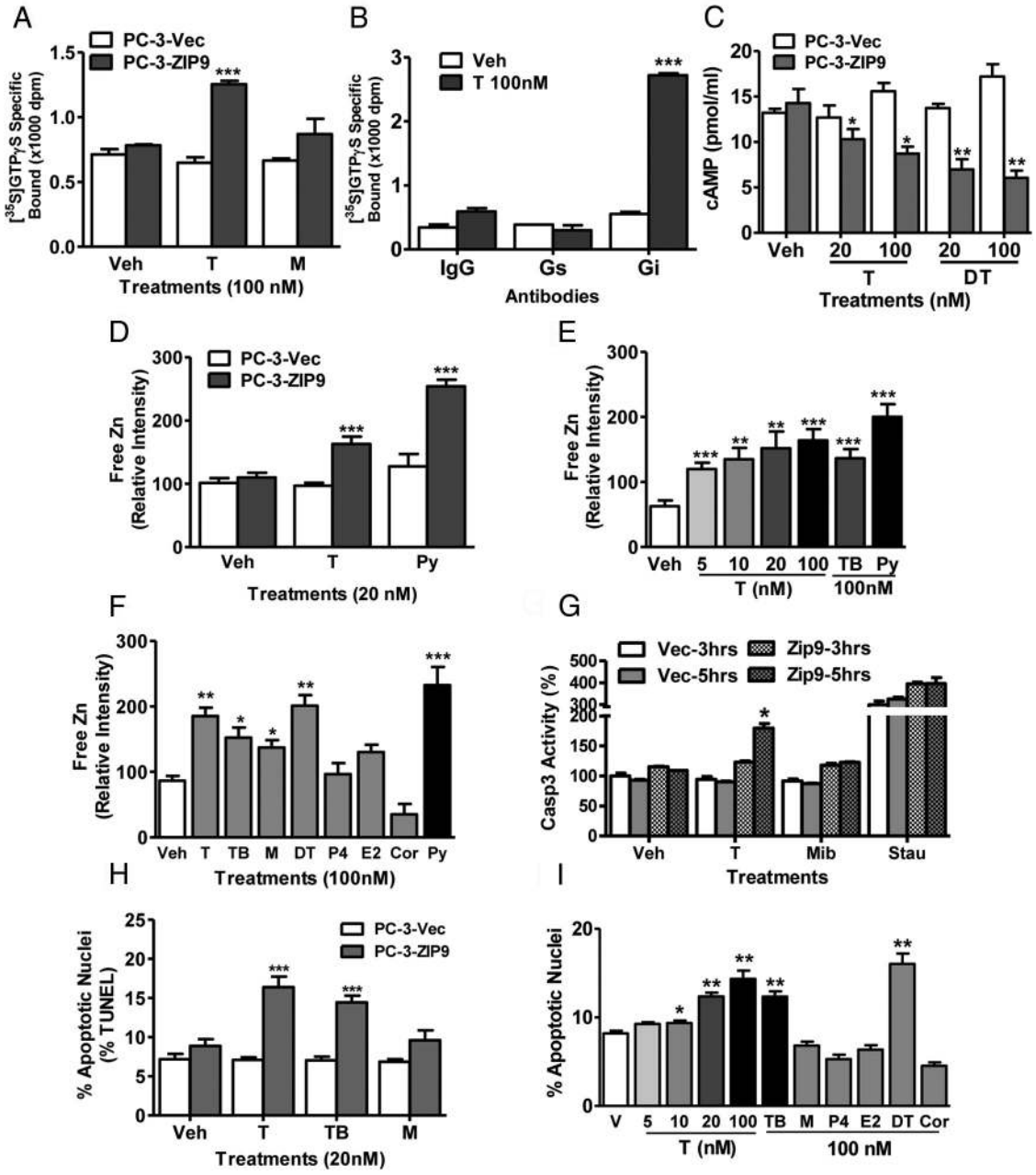

Figure 4. Effects androgens on signal transduction pathways and apoptosis in PC-3 human prostate cancer cells overexpressing ZIP9 (PC-3-ZIP9) and in cells transfected with vector alone (PC-3-Vec). A, Effects of treatments with (100nM) testosterone (T) and mibolerone (M) on [^{35}S]-GTPγS binding to plasma membranes. ***, $P < .001$ compared with vehicle (Veh) control, n = 6. B, Immunoprecipitation of [^{35}S]-GTPγS bound to G protein α-subunits proteins on plasma membranes activated by 100nM T treatment with specific Gα-subunit antibodies or control IgG. Gs, $G_{\alpha s}$ antibody, Gi, $G_{\alpha i}$ antibody. ***, $P < .001$ compared with corresponding IgG control, n = 6. C, Effects of 20 minutes of treatments with T and dihydrotestosterone (DT) (20nM, 100nM) on cAMP production. **, $P < .01$; *, $P < .05$ compared with corresponding PC-3-Vec control. D–F, Effects of T and other steroid treatments on relative intracellular free zinc levels. D, Effects of 20nM T treatment on zinc levels in PC-3-ZIP9 and PC-3-Vec cells. ***, $P < .001$; **, $P < .01$ compared with corresponding PC-3-Vec controls. E, Concentration-dependent effects of T and effects of T-BSA on zinc levels in PC-3-ZIP9 cells. ***, $P < .001$; **, $P < .01$ compared with Veh controls. F, Effects of different steroid treatments (100nM) on intracellular zinc concentrations in PC-3-ZIP9 cells. Py, pyrithione-positive control; TB, T conjugated to bovine serum albumen. ***, $P < .001$; **, $P < .01$; *, $P < .05$ compared with Veh control. G, Effects of treatment with 20nM T and M for 3 and 5 hours on of Caspase 3 activity. Stau, staurosporin. *, $P < .05$ compared with respective Veh control H and I. Effects of T and other steroids on % apoptotic nuclei by TUNEL (H) and Hoechst (I), in PC-3-ZIP9 cells assays. ***, $P < .001$; **, $P < .01$; *, $P < .05$ compared with respective Veh controls, n = 6 (see Figure 1 for key to steroid abbreviations).

cells (Figure 4H). Testosterone caused a concentration-dependent potentiation of serum starvation-induced apoptosis in PC-3-ZIP9 cells over the range of 10nM to 100nM, an effect mimicked with 100nM testosterone-BSA and dihydrotestosterone, but not by mibolerone, progesterone, and cortisol (Figure 4I).

[^{3}H]-T binding and testosterone induction of signaling and apoptosis through ZIP9 in LNCaP cells and in ZIP9-transfected MDA-MB-231 cells

Comparable results were obtained in nAR-positive LNCaP human prostate cancer cells, and triple-negative MDA-MB-231 cells stably transfected with ZIP9 (MDA-MB-231-ZIP9) (Figure 5). LNCaP cells showed moderate expression of ZIP9 protein, which was almost completely eliminated after transient transfection of ZIP9 siRNA (Figure 5A, top) and was accompanied by a significant decline in specific [^{3}H]-T binding compared with untreated and nontarget siRNA controls (Figure 5A, bottom). Testosterone treatments caused significant increases in intracellular zinc concentrations and apoptosis in cells transfected with the nontarget siRNA, whereas these testosterone actions were completely blocked after transfection with ZIP9 siRNA (Figure 5, B and C). Relatively weak plasma membrane expression of ZIP9 in MDA-MB-231

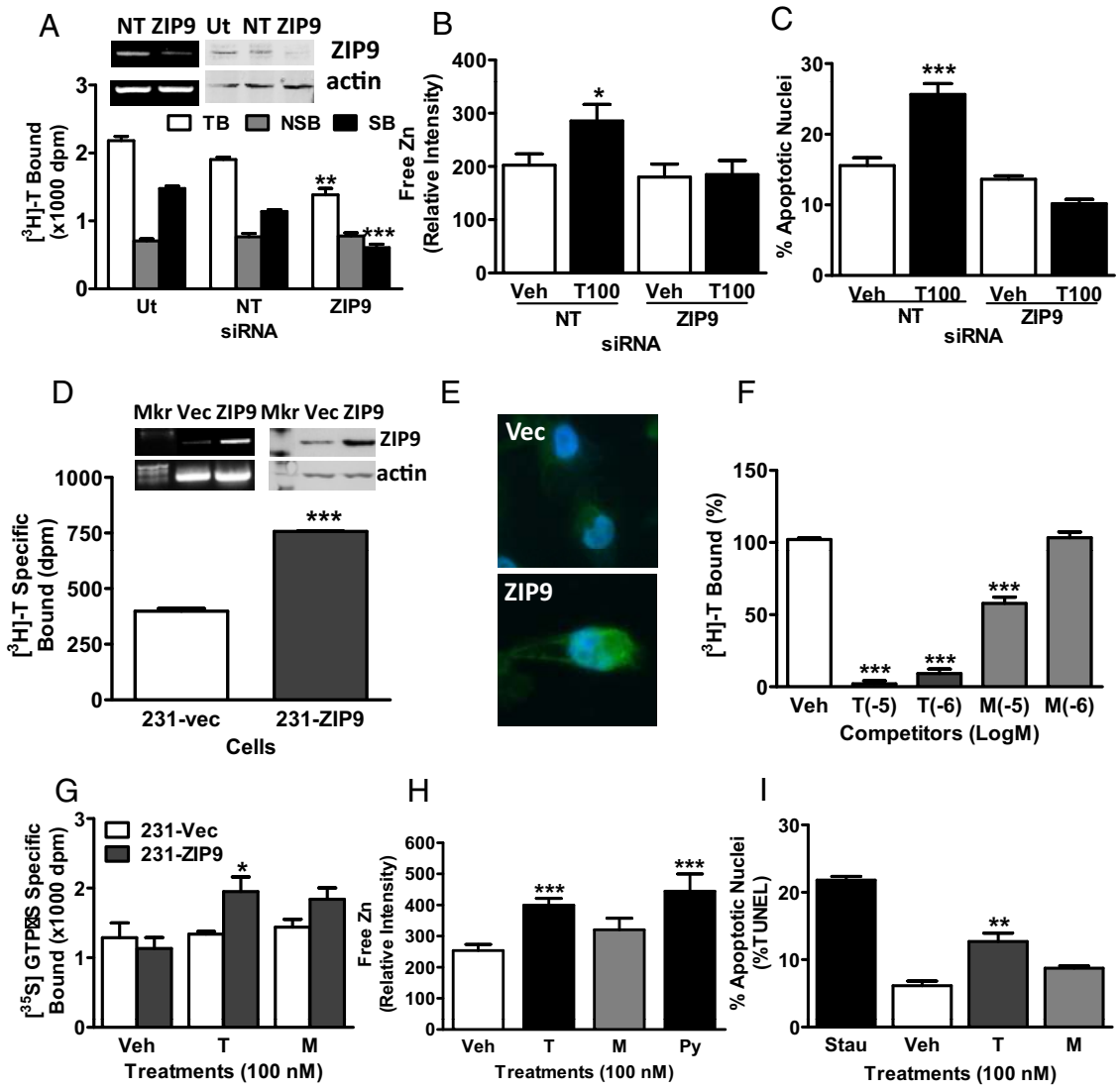

Figure 5. Membrane testosterone (T) binding and effects of androgens on signal transduction pathways and apoptosis in AR-positive human LNCaP prostate cancer cells (A–C) and in triple-negative MDA-MB-231 breast cancer cells (D–I) overexpressing ZIP9 (231-ZIP9) or vector alone (231-Vec). A–C, Effects of transfection of LNCaP cells with ZIP9 siRNA (ZIP9) or nontarget (NT) siRNA on ZIP9 mRNA (A, top, left) and protein (A, top, right) expression, and specific [^{3}H]-T binding in a single-point binding assay. Ut, untransfected cells; actin, actin loading control. TB, total binding; NSB, nonspecific binding; SB, specific binding. ***, $P < .001$; **, $P < .01$ compared with their respective NT controls, n = 6 (A, bottom); on relative intracellular free zinc concentrations, *, $P < .05$ compared with NT vehicle (Veh) control (B); and on % apoptotic nuclei, ***, $P < .001$ compared with NT Veh control (C). D, Expression of ZIP9 mRNA (top, left) and protein on plasma membrane (top, right) and specific [^{3}H]-T binding in a single-point binding assay (bottom) in 231-ZIP9 and in 231-vec cells. ***, $P < .001$ compared with 231-vec control. E, Immunocytochemical analysis of ZIP9 protein expression in 231-vec (Vec) and 231-ZIP9 (ZIP9) cells. F, Two-point competitive binding assay of T and mibolerone (M) (100nM and 1μM, respectively) binding to 231-ZIP9 cell membranes expressed as a percentage of maximum specific [^{3}H]-T-binding. ***, $P < .001$ compared with Veh control. G–I, Effects of T and M (100nM) on [^{35}S]GTPγS binding to plasma membranes (G), on intracellular zinc concentrations in 231-ZIP9 cells (H), and on % apoptotic nuclei in 231-ZIP9 cells (I). Py, pyrithione-positive zinc control; Stau, staurosporine-positive apoptosis control. ***, $P < .001$; **, $P < .01$; *, $P < .05$ compared with respective Veh controls, n = 6.

cells was increased after stable transfection of ZIP9 (Figure 5, D, top, and E, bottom) and was accompanied by an approximately 2-fold increase in specific [^{3}H]-T binding (Figure 5D, bottom). Two-point competitive binding assays showed that 100nM and 1μM testosterone caused almost complete displacement of [^{3}H]-T binding to MDA-MB-231-ZIP9 cell membranes, whereas mibolerone was less effective as a competitor (Figure 5F). Treatment with testosterone but not with mibolerone caused G protein activation in MDA-MB-231-ZIP9 cells but not in vector-transfected cells (Figure 5G). Similar to results with the other cell lines, treatment with testosterone also increased intracellular free zinc concentrations and percent apoptotic nuclei in MDA-MB-231-ZIP9 cells (Figure 5, H and I).

Testosterone up-regulation of apoptotic pathways in MDA-MB-468 and PC-3-ZIP9 cells

Effects of treatment with 20nM testosterone on expression of genes in the intrinsic apoptotic pathway, Bax and p53, as well as JNK, which participates in both intrinsic and extrinsic apoptotic pathways, were investigated in MDA-MB-468 and PC-3-ZIP9 cells. Treatment of serum-starved PC-3-ZIP9 cells for 24 hours with 20nM testosterone caused significant up-regulation of Bax, p53, and JNK mRNAs, whereas this treatment was ineffective in PC-3-Vec cells (Figure 6, A–C). Similarly, testosterone treatment (20nM) increased expression of all 3 genes in MDA-MB-468 cells (Figure 6, D–F). Treatment for 48 hours with 20nM testosterone increased expression of Bax, Caspase 3, and cytochrome C proteins in both MDA-MB-468 cells and PC-3-ZIP9 cells compared with vehicle-treated controls, whereas no changes were observed in the PC-3-Vec cells (Figure 6, G–I).

Testosterone up-regulation of apoptotic genes in MDA-MB-468 and PC-3-ZIP9 cells through ERK- and zinc-dependent pathways

Involvement of testosterone-induced increases in intracellular zinc and activation of MAPK in mediating increases in Bax, p53, and JNK mRNA expression were investigated in MDA-MB-468 and PC-3-ZIP9 cells, respectively. Pretreatment for 24 hours with the zinc chelator TPEN (N,N,N′,N′-Tetrakis(2-pyridylmethyl)ethylenediamine) did not significantly affect expression of the apoptotic genes alone in MDA-MB-468 cells but greatly attenuated the 20nM testosterone-induced increase in their expression (Figure 7, A–C). Similarly, although MAPK inhibitor PD98059 (2-(2-Amino-3-methoxyphenyl)-4H-1-benzopyran-4-one) (10μM) treatment alone did not alter gene expression, it completely blocked the stimulatory effect of 20nM testosterone on Bax, p53, and JNK mRNA expression in PC-3-ZIP9 cells (Figure 7, D–F).

ZIP9 expression in cell lines and in normal and malignant human tissues

ZIP9 was detected by q-PCR in all human tissues and cells examined (Figure 7, G and H). Relative ZIP9 mRNA expression was high in pancreas, testis, and pituitary and intermediate in the kidney, liver, uterus, heart, prostate, and brain, whereas expression was lower in the ovary and colon (Figure 7G). Relative ZIP9 mRNA expression was high in MDA-MB-468, LNCaP, T47D, and Jurkat cells, intermediate in PC-3 cells, MDA-MB-231, and SKBR3 cells, which were used for recombinant expression of human and croaker ZIP9s, respectively, and low in noncancer vascular endothelial and smooth muscle cells and granulosa cells (Figure 7H). ZIP9 mRNA expression was significantly greater in biopsies of human malignant prostate tissues compared with that in paired normal prostate tissue collected from 4 patients (Figure 8A), which was also apparent when the results were combined (Figure 8B). ZIP9 mRNA expression was significantly up-regulated in malignant human breast tissue compared with normal tissue from the same breast in paired biopsy samples from 5 out of 6 patients (Figure 8C), which was also significantly higher when results of the 6 patients were combined (Figure 8D). Immunohistochemical analysis of both normal and malignant prostate and breast tissue biopsy samples collected from these patients showed increased expression of ZIP9 protein in malignant tissues (Figure 8E and Supplemental Figure 2). Relatively weak immunostaining with the human nAR antibody was also detected in these normal tissue biopsies, which was not significantly increased in the malignant tissues (Figure 8E and Supplemental Figure 2).

Discussion

The present results provide convincing evidence that a zinc transporter protein belonging to the ZIP (SLC39A) family, ZIP9, functions as a mAR in mammalian cells. Results of both gain of function experiments in PC-3 and MDA-MB-231 cells overexpressing ZIP9 and knockdown studies in MDA-MB-468 cells and LNCaP cells treated with ZIP9 siRNA strongly support this conclusion. The discovery that human ZIP9 displays high-affinity (K_d, 14.4nM), limited capacity (B_{max}, 7.4nM/mg protein), displaceable, specific, membrane [^{3}H]-T binding characteristic of a mAR corroborates previous results with Atlantic croaker ZIP9. Furthermore, the finding that testosterone activates G proteins and increases intracellular free zinc concentrations

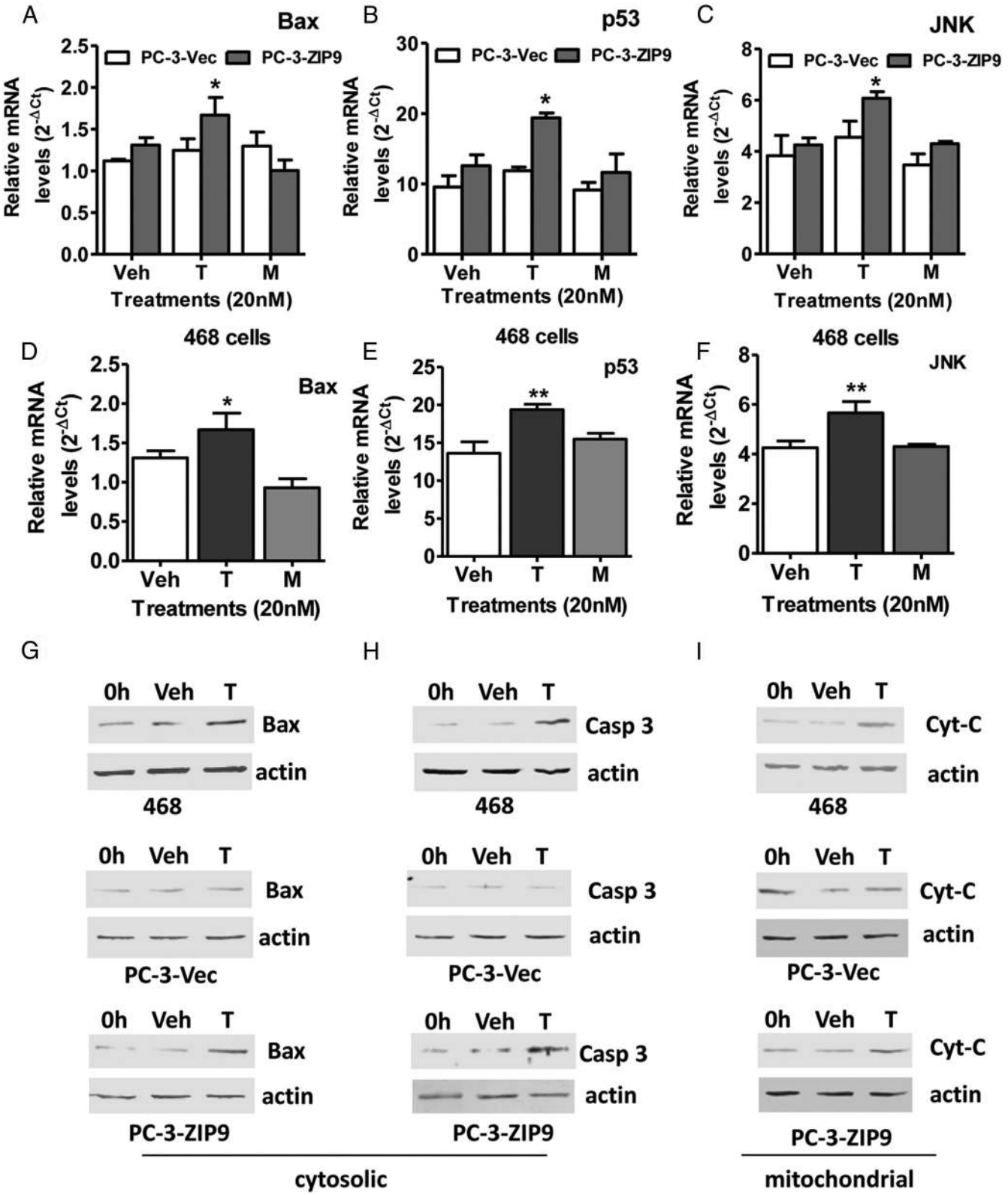

Figure 6. Effects of testosterone (T) and mibolerone treatments on expression of members of apoptotic pathways in MDA-MB-468 (468), PC-3-ZIP9 and PC-3-Vec cells. A–F, Effects of 24-hour treatments with 20nM T and mibolerone on relative mRNA levels of Bax, p53, and JNK in PC-3-ZIP9 and PC-3-Vec (A–C) and in MDA-MB-468 (D–F) cells measured by q-PCR. **, $P < .01$ compared with vehicle (Veh) controls; *, $P < .05$ compared with corresponding PC-3-Vec treatments or Veh control, n = 6. G–I, Effects of 48 hours of treatment with 20nM T or Veh, or 0 hours of no treatment (0 h) on cytosolic expression of Bax and Caspase 3 (Casp3) proteins, and mitochondrial expression of cytochrome C (Cyt-C) protein in MDA-MB-468, PC-3-ZIP9, and PC-3-Vec cells determined by Western blot analysis. Actin, actin loading control.

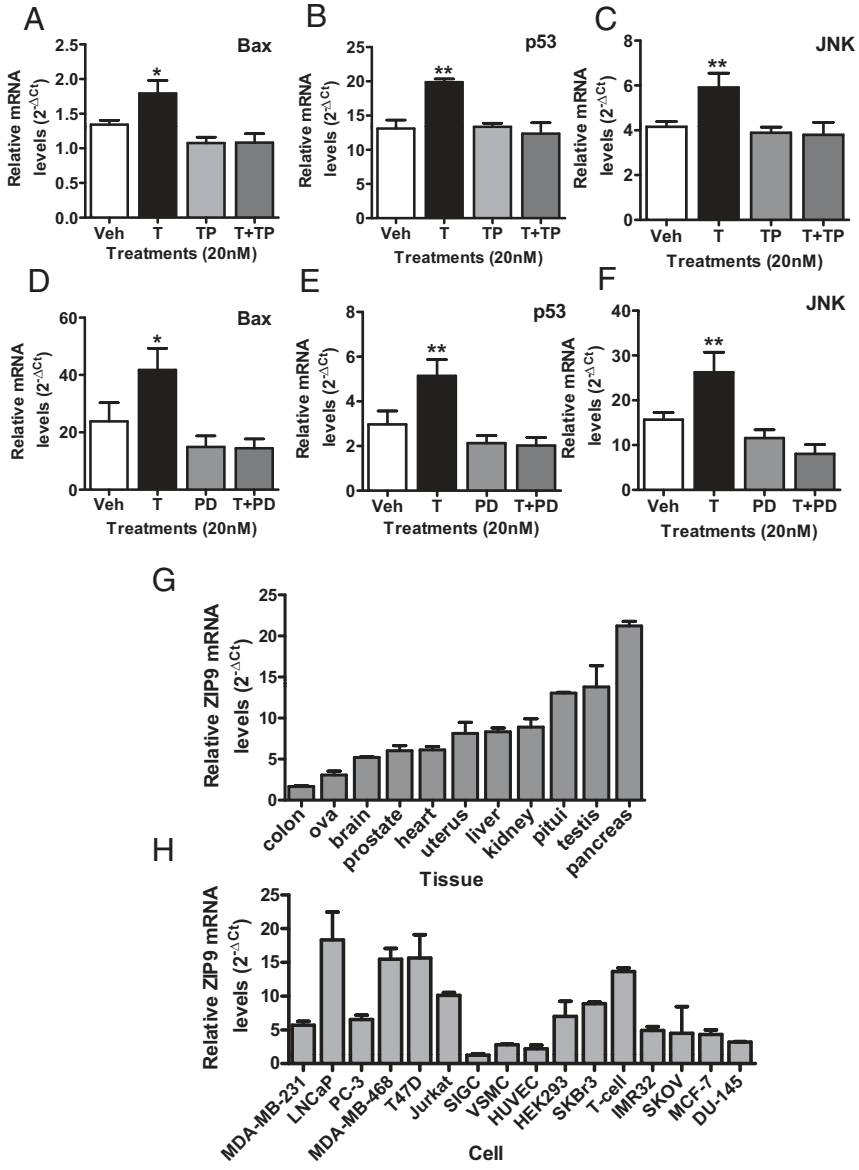

Figure 7. Effects of cotreatment with an intracellular zinc chelator (TPEN) or a MAPK inhibitor (PD98059) on testosterone (T) (20nM) up-regulation of Bax, p53, and JNK mRNA expression in MDA-MB-468 (A–C) and PC-3-ZIP9 (D–F) cells after 24 hours of treatment. Veh, vehicle; TP, TPEN; PD, PD98059. **, $P < .01$; *, $P < .05$ compared with respective Veh controls. G, Relative expression of ZIP9 mRNA in normal adult human RNA samples. Pitui, pituitary; n = 3. H, Relative ZIP9 mRNA expression in cancer and noncancer cells. Cancer cell lines: MDA-MB-231, MDA-MB-468, SKBR3, T47D, and MCF-7 (breast); LNCaP, PC-3, and DU-145 (prostate); SKOV (ovarian); IMR-32 (neuroblastoma, brain); and Jurkat (T-cell leukemia). Noncancer cells: SIGC (spontaneously immortalized granulosa cells; using rat ZIP9 primers); VSMC (primary vascular smooth muscle cells from human umbilical vein); HUVEC (primary endothelial cells from human umbilical vein); T-cell (human T lymphocytes); and HEK293.

through human ZIP9 indicates that the signal transduction pathways mediated by human and croaker ZIP9s are similar. Finally, testosterone regulates the same cellular functions in a mammalian and teleost species, inducing apoptosis through ZIP9s in both human and croaker cells. The identification of shared mAR and proapoptotic functions of ZIP9s in teleost fish and mammals, which diverged approximately 450 million years ago, suggests that androgen signaling to regulate apoptosis is a fundamental, conserved function of ZIP9 in vertebrates and probably its primary physiological role.

Human ZIP9 differs from croaker ZIP9 in its high relative binding affinity for progesterone. However, progesterone does not activate ZIP9, because it did not increase intracellular zinc concentrations or induce apoptosis. Similarly, the potent nAR agonist, mibolerone, was ineffective in activating ZIP9-dependent signaling pathways, and in inducing apoptosis and up-regulation of proapoptotic genes in the cancer cells, suggesting that it will be a useful tool for distinguishing nAR-dependent androgen actions from those mediated through ZIP9. The finding that the nonaromatizable androgen dihydrotestosterone mimicked the effects of testosterone in these cancer cells, whereas estradiol-17β had negligible binding affinity and activity, does not support a role for aromatization in these androgen actions. Androgen actions on intracellular zinc concentrations and apoptosis are initiated at the cell surface, because they are mimicked by the membrane-impermeable testosterone conjugate, testosterone-BSA. Taken together, these results demonstrate that ZIP9 is specifically activated by androgens and functions as a mAR on the cell surface of human breast cancer and prostate cancer cells.

The demonstration that testosterone treatment of MDA-MB-468 and PC-3-ZIP9 cells causes G protein activation further supports the proposed role of human ZIP9 as a mAR. Moreover, down-regulation of cAMP production in PC-3-ZIP9 cells is consistent with immunoprecipitation results showing that testosterone activates an inhibitory G protein in these cells, presumably through the G protein α-subunit. The $\beta\gamma$ G protein subunit also appears to be involved in ZIP9 signaling, because testosterone causes phosphorylation of ERK in MDA-MB-468 cells. In addition to mediating testosterone signaling typical of a mAR,

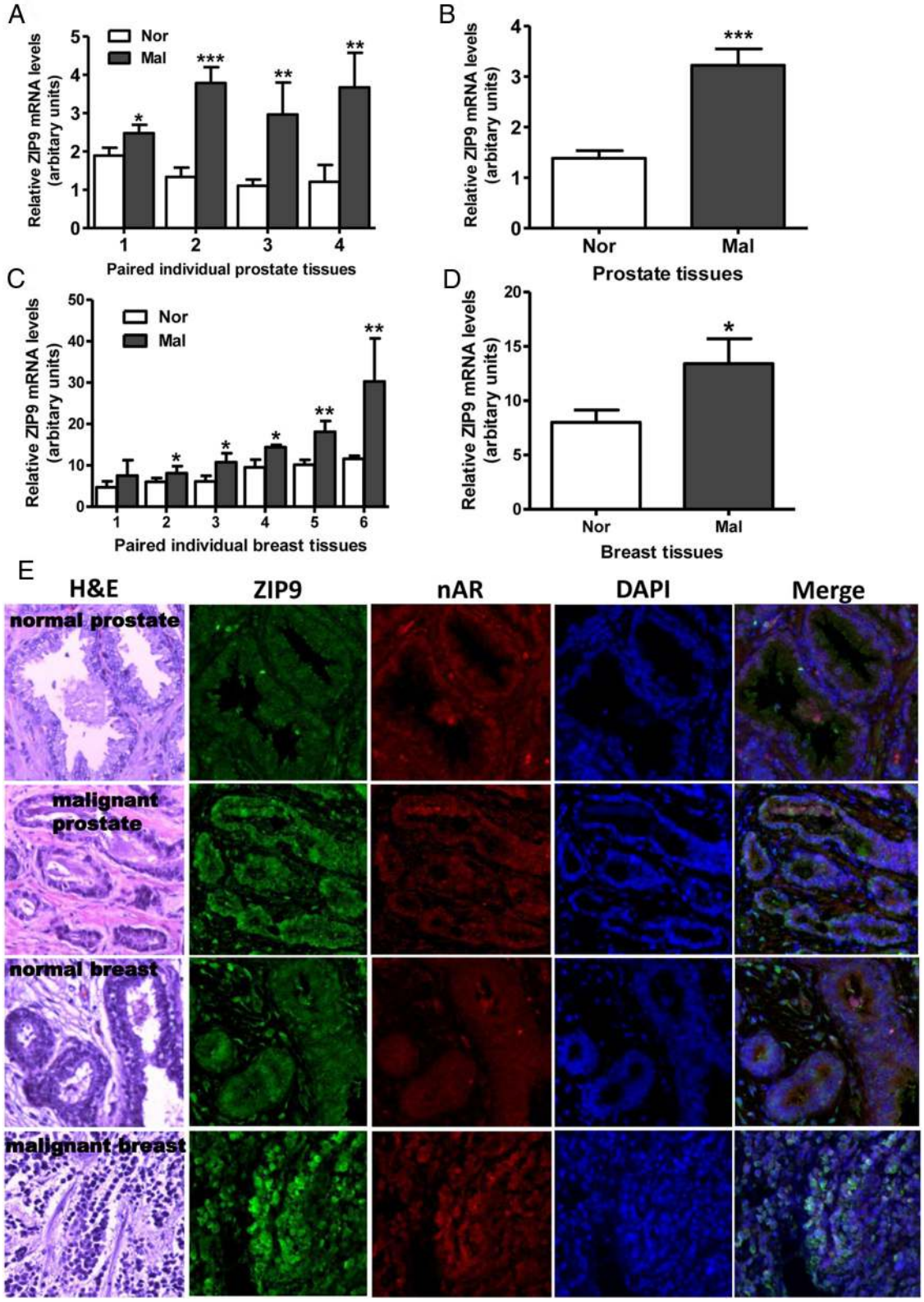

Figure 8. Relative expression of ZIP9 mRNA in paired normal (Nor) and malignant (Mal) human prostate (A and B) and breast (C and D) tissue biopsies measured by q-PCR. ***, $P < .001$; **, $P < .01$; *, $P < .05$ compared with respective paired normal control (A and C) or respective mean normal controls (B and D). All the malignant prostate biopsy samples were classified as acinar adenocarcinoma (Gleason score 6–7). All the malignant breast biopsy specimens were classified as invasive ductal carcinoma (Nottingham grade 3 or Bloom-Richardson 2–3) (see Supplemental Table 2 for additional details of the malignant biopsy samples). E, Hematoxylin and eosin (H&E) staining and immunohistochemistry of representative normal and malignant prostate (biopsy specimen 1) and breast cancer (biopsy specimen 3) tissues showing localization of ZIP9 and nAR proteins (see Supplemental Figure 2 for additional immunohistochemistry images of these specimens). Image amplification, ×100.

ZIP9 also functions like other ZIPs as a zinc transporter, increasing intracellular free zinc concentrations. However, the zinc transport function of ZIP9 differs from that currently known for all other members of the ZIP family in that it is acutely up-regulated within 30 minutes by physiologically relevant concentrations of steroid hormones acting at the cell surface. Importantly, the androgen specificity of this zinc up-regulation closely matches that for ligand binding to ZIP9 mAR, suggesting a close association between these 2 distinct functions of ZIP9, although the nature of this interaction remains unclear.

None of the other 13 ZIP family members are obvious candidates for steroid membrane receptors, because ZIP9 is not closely related to any of them and is the sole member of ZIP subfamily I (37, 38). Nevertheless, evidence has gradually emerged from disparate clinical and experimental studies for hormonal regulation of zinc homeostasis and expression of several ZIP genes (28, 45). For example, sex differences in zinc levels have been reported in murine cerebral cortex synaptic vesicles (46), which are related to sex differences in the severity of histopathology in a murine model of Alzheimer's disease (47). Both androgens and estrogens have been shown to modulate zinc homeostasis in mouse brain, but the mechanisms are not known (48). Sex differences have also been observed in steroid regulation of zinc uptake by murine small intestine (49). Prolactin and testosterone treatments regulate a zinc transporter in prostate cancer cells (50) reported to be ZIP1 (28), and treatment of MCF-7 breast cancer cells with estradiol-17β for 7 days was reported to increase ZIP6 and ZIP14 mRNA levels, whereas treatment with the antiestrogen, fulvestrant, decreased the expression of these genes (51). Our results show that ZIP9 expression in MDA-MB-468 cells and in croaker ovaries (64) is also up-regulated after incubation with steroid hormones. These hormone-induced increases in membrane ZIP9 expression are likely to be of physiological significance, because in both cases, they were accompanied by enhanced mAR function, shown as increased receptor binding.

One function of ZIP9 clearly identified in this study is its role as an intermediary in testosterone induction of apoptosis in human breast and prostate cancer cells. This function of ZIP9 is not limited to immortalized cancer cells, because it has also been demonstrated in primary cultures of croaker granulosa and theca cells (64). The ZIP9 signaling mediating apoptosis in both breast cancer and prostate cancer cells includes genomic actions, because the key proapoptotic genes, Bax, p53, and JNK (52–54), were all significantly up-regulated by testosterone treatment. An interesting finding is that these testosterone-induced increases in mRNA expression are blocked when either mAR signaling or zinc transporter signaling functions of ZIP9 are attenuated by treatment with a MAPK inhibitor (PD98059) and a zinc chelator (TPEN), respectively. An intriguing possibility that will require further interrogation is that ERK phosphorylation and increases in cytosolic free zinc are components of a single signaling pathway regulating expression of apoptotic genes. The observation that testosterone treatment increases Bax, cytochrome C, and Caspase 3 protein expression in both cell lines indicates that ZIP9 activates the mitochondrial apoptotic (intrinsic) pathway (52). It is noteworthy that the same mitochondrial apoptogenic pathway is induced in PC-3 cells by incubation in media with elevated concentrations of zinc, 15μM, 10-fold higher than that used in the present study (55, 56). The finding that apoptosis is induced in nAR-negative MDA-MB-468, MDA-MB-231, and PC-3-ZIP9 cells by a cell-surface action of testosterone is in agreement with previous studies indicating it is mediated through a mAR in a nAR-deficient prostate cancer cell (DU-145) line (24, 57). Similar to our results in MDA-MB-468 cells, the apoptotic response to testosterone in T47D breast cancer cells involves a pertussis toxin-sensitive inhibitory G protein and activation of MAPK (58). Apoptotic responses identified in DU-145 cells, involving down-regulation of PI3K/Akt (phosphatidylinositol 3-kinase/serine/threonine kinase Akt) and NF-κB (nuclear factor kappa-light-chain-enhancer of activated B cells) activity and increased FasL (Fas ligand) expression and Bad (Bcl-2-associated death promoter) protein activity (57), have not been investigated through ZIP9 in prostate cancer cells, so it is not known whether testosterone promotion of cell death through ZIP9 also involves the extrinsic (death receptor-mediated) apoptotic pathway.

An initial survey of ZIP9 expression in malignant breast and prostate biopsy samples suggests that it is up-regulated in malignant cells. The finding that ZIP9 mRNA expression is up-regulated in both malignant breast and prostate tissues is in agreement with previous immunohistochemistry results (59) and has been reported for ZIP6, ZIP7, and ZIP10 in breast cancer tissues (51), although other ZIPs (ZIP1, ZIP2, and ZIP3) are down-regulated in prostate cancer tissues (60). Increases in ZIP expression in most cancers are suggested to be related to an increase in zinc requirements in rapidly dividing cells (61). Indeed, highest expression of the ZIP9 protein was detected in invasive epithelial cells in the breast cancer biopsies and in the glandular epithelial cells in the prostate cancer samples, sites of proliferation in invasive ductal carcinoma, and in prostate gland tumorigenesis, respectively (62, 63). This suggests that ZIP9 is a potential therapeutic target for treating breast and prostate cancers and an intriguing possibly is that treatment with a specific ZIP9 agonist would selectively cause apoptosis and death

of the malignant cells in these tumors. However, these preliminary results first need to be confirmed in additional cancer biopsy samples representing a broader range of cancer grades and subjected to comprehensive histopathological analyses of ZIP9 expression.

In conclusion, novel steroid signaling pathways initiated through the zinc transporter ZIP9 protein have been identified on cell membranes of cancer cells that mediate androgen promotion of apoptosis. The discovery that a single protein performs dual functions as an mAR and zinc transporter in mammalian cells indicates that a previously unrecognized intimate relationship exists between steroid and zinc signaling pathways.

Acknowledgments

We thank a clinical pathologist, Dr Xinzhu Pang, for assistance in selecting images of the malignant prostate and breast biopsies and for confirming the presence of invasive cancer cells.

Address all correspondence and requests for reprints to: Peter Thomas, Marine Science Institute, The University of Texas at Austin, 750 Channel View Drive, Port Aransas, TX 78373. E-mail: peter.thomas@utexas.edu.

This work was supported by the National Institutes of Health Grant ESO 12961 (to P.T.).

Disclosure Summary: The authors have nothing to disclose.

References

1. **Revelli A, Massobrio M, Tesarik J.** Nongenomic actions of steroid hormones in reproductive tissues. *Endocr Rev*. 1998;19:3–17.
2. **Thomas P.** Rapid steroid hormone actions initiated at the cell surface and the receptors that mediate them with an emphasis on recent progress in fish models. *Gen Comp Endocrinol*. 2012;175:367–383.
3. **Norman AW, Mizwicki MT, Norman DP.** Steroid-hormone rapid actions, membrane receptors and a conformational ensemble model. *Nat Rev Drug Discov*. 2004;3:27–41.
4. **Chambliss KL, Yuhanna IS, Anderson RG, Mendelsohn ME, Shaul PW.** Rβ has nongenomic action in caveolae. *Mol Endocrinol*. 2002; 16:938–946.
5. **Yang X, Guo Z, Sun F, et al.** Novel membrane-associated androgen receptor splice variant potentiates proliferative and survival responses in prostate cancer cells. *J Biol Chem*. 2011;286:36152–36160.
6. **Boonyaratanakornkit V, Scott MP, Ribon V, et al.** The role of extranuclear signaling actions of progesterone receptor in mediating progesterone regulation of gene expression and the cell cycle. *Mol Endocrinol*. 2007;21:359–375.
7. **Nadal A, Ropero AB, Laribi O, Maillet M, Fuentes E, Soria B.** Nongenomic actions of estrogens and xenoestrogens by binding at a plasma membrane receptor unrelated to estrogen receptor α and estrogen receptor β. *Proc Natl Acad Sci USA*. 2000;97:11603–11608.
8. **Frye CA, Sumida K,Lydon JP, O'Malley BW, Pfaff DW.** Mid-aged and aged wild-type and progestin receptor knockout (PRKO) mice demonstrate rapid progesterone and 3α, 5α-THP-facilitiated lordosis. *Psychopharmacology*. 2006;185:423–432.
9. **Benten WP, Lieberherr M, Giese G, et al.** Functional testosterone receptors in plasma membranes of T cells. *FASEB J*. 1999;13:123–133.
10. **Zhu Y, Rice CD, Pang Y, Pace M, Thomas P.** Cloning, expression, and characterization of a membrane progestin receptor and evidence it is an intermediary in meiotic maturation of fish oocytes. *Proc Natl Acad Sci USA*. 2003;100:2231–2236.
11. **Zhu Y, Bond J, Thomas P.** Identification, classification, and partial characterization of genes in humans and other vertebrates homologous to a fish membrane progestin receptor. *Proc Natl Acad Sci USA*. 2003;100:2237–2242.
12. **Thomas P, Pang Y, Filardo EJ, Dong J.** Identity of a membrane estrogen receptor coupled to a G protein in human breast cancer cells. *Endocrinology*. 2005;146:624–632.
13. **Revankar CM, Cimino DF, Sklar LA, Arterburn JB, Prossnitz ER.** A transmembrane intracellular estrogen receptor mediates rapid cell signaling. *Science*. 2005;307:1625–1630.
14. **Rahman F, Christian HC.** Non-classical actions of testosterone: an update. *Trends Endocrinol Metab*. 2008;18:371–378.
15. **Foradori CD, Weiser MJ, Handa RJ.** Non-genomic actions of androgens. *Front Neuroendocrinol*. 2008;29:169–181.
16. **Machelon V, Nomé F, Tesarik J.** Nongenomic effects of androstenedione on human granulosa luteinizing cells. *J Clin Endocrinol Metab*. 1998;83:263–269.
17. **Liu D, Dillon JS.** Dehydroepiandrosterone activates endothelial cell nitric-oxide synthase by a specific plasma membrane receptor coupled to Gα(i2,3). *J Biol Chem*. 2002;277:21379–21388.
18. **Braun AM, Thomas P.** Androgens inhibit estradiol-17β synthesis in Atlantic croaker (*Micropogonias undulatus*) ovaries by a nongenomic mechanism initiated at the cell surface. *Biol Reprod*. 2003; 69:1642–1650.
19. **Sun YH, Gao X, Tang YJ, Xu C-L, Wang LH.** Androgens induce increases in intracellular calcium via a G protein-coupled receptor in LNCaP prostate cancer cells. *J Androl*. 2006;27:671–678.
20. **Armen TA, Gay CV.** Simultaneous detection and functional response of testosterone and estradiol receptors in osteoblast plasma membranes. *J Cell Biochem*. 2000;79:620–627.
21. **Lieberherr M, Grosse B.** Androgens increase intracellular calcium concentration and inositol 1,4,5-trisphosphate and diacylglycerol formation via a pertussis toxin-sensitive G-protein. *J Biol Chem*. 1994;269:7217–7223.
22. **Benten WP, Lieberherr M, Stamm O, Wrehlke C, Guo Z, Wunderlich F.** Testosterone signaling through internalizable surface receptors in androgen receptor-free macrophages. *Mol Biol Cell*. 1999; 10:3113–3123.
23. **Leung GP, Cheng-Chew SB, Wong PY.** Nongenomic effect of testosterone on chloride secretion in cultured rat efferent duct epithelia. *Am J Physiol Cell Physiol*. 2001;280:C1160–C1167.
24. **Hatzoglou A, Kampa M, Kogia C, et al.** Membrane androgen receptor activation induces apoptotic regression of human prostate cancer cells *in vitro* and *in vivo*. *J Clin Endocrinol Metab*. 2005;90: 893–903.
25. **Guo Z, Benten WP, Krücken J, Wunderlich F.** Nongenomic testosterone calcium signaling. Genotropic actions in androgen receptor-free macrophages. *J Biol Chem*. 2002;277:29600–29607.
26. **Kelder J, Azevedo R, Pang Y, de Vlieg J, Dong J, Thomas P.** Comparison between steroid binding to membrane progesterone receptor α (mPRα) and to nuclear progesterone receptor: correlation with physicochemical properties assessed by comparative molecular field analysis and identification of mPRα-specific agonists. *Steroids*. 2010;75:314–322.
27. **Bologa CG, Revankar CM, Young SM, et al.** Virtual and biomolecular screening converge on a selective agonist for GPR30. *Nat Chem Biol*. 2006;2:207–212.

28. **Cousins RJ, Liuzzi JP, Lichten LA.** Mammalian zinc transport, trafficking, and signals. *J Biol Chem*. 2006;281:24085–24089.
29. **Solomons NW.** Update on zinc biology. *Ann Nutr Metab*. 2013; 62:8–17.
30. **Jackson KA, Valentine RA, Coneyworth LJ, Mathers JC, Ford D.** Mechanisms of mammalian zinc-regulated gene expression. *Biochem Soc Trans*. 2008;36:1262–1266.
31. **Vallee BL, Auld DS.** Zinc coordination, function, and structure of zinc enzymes and other proteins. *Biochemistry*. 1990;29:5647–5659.
32. **Formigari A, Irato P, Santon A.** Zinc, antioxidant systems and metallothionein in metal-mediated apoptosis: biochemical and cytochemical aspects. *Comp Biochem Physiol C*. 2007;146:443–459.
33. **Hasse H, Rink L.** Functional significance of zinc-related signaling pathways in immune cells. *Ann Rev Nutr*. 2009;29:133–152.
34. **Jeong J, Eide DJ.** The SLC39 family of zinc transporters. *Mol Aps Med*. 2013;34:612–619.
35. **Wenzlau JM, Juhl K, Yu L, et al.** The cation efflux transporter ZnT8 (SLC30A8) is a major autoantigen in human type 1 diabetes. *Proc Natl Acad Sci USA*. 2007;104:17040–17045.
36. **Franklin RB, Feng P, Milon B, et al.** hZIP1 zinc uptake transporter turnover down regulation and zinc depletion in prostate cancer. *Mol Cancer*. 2005;4:32.
37. **Fukada T, Kambe T.** Molecular and genetic features of zinc transporters in physiology and pathogenesis. *Metallomics*. 2011;3:662–674.
38. **Matsuura W, Yamazaki T, Yamaguchi-Iwai Y, et al.** SLC39A9 (ZIP9) regulates zinc homeostasis in the secretory pathway: characterization of the ZIP subfamily I protein in vertebrate cells. *Biosci Biotechnol Biochem*. 2009;73:1142–1148.
39. **Taniguchi M, Fukunaka A, Hagihara M, et al.** Essential role of the zinc transporter ZIP9/SLC39A9 in regulating the activations of Akt and Erk in B-cell receptor signaling pathway in DT40 cells. *PLoS One*. 2013;8(3):e58022.
40. **Papadopoulou N, Papakonstanti EA, Kallergi G, et al.** Membrane androgen receptor activation in prostate and breast tumor cells: molecular signaling and clinical impact. *IUBMB Life*. 2009;61:56–61.
41. **Pang Y, Dong J, Thomas P.** Characterization, neurosteroid binding and brain distribution of human membrane progesterone receptors δ and ϵ (mPRδ and mPRϵ) and mPRδ involvement in neurosteroid inhibition of apoptosis. *Endocrinology*. 2013;154:283–295.
42. **Filardo E, Quinn J, Pang Y, et al.** Activation of the novel estrogen receptor G protein-coupled receptor 30 (GPR30) at the plasma membrane. *Endocrinology*. 2007;148:3236–3245.
43. **Braun AM, Thomas P.** Biochemical characterization of a membrane androgen receptor in the ovary of the Atlantic croaker (*Micropogonias undulatus*). *Biol Reprod*. 2004;71:146–155.
44. **Merten KE, Jiang Y, Kang YJ.** Zinc inhibits doxorubicin-activated calcineurin signal transduction pathway in H9c2 embryonic rat cardiac cells. *Exp Biol Med (Maywood)*. 2007;232:682–689.
45. **el-Tanani MK, Green CD.** Oestrogen-induced genes, pLIV-1 and pS2, respond divergently to other steroid hormones in MCF-7 cells. *Mol Cell Endocrinol*. 1995;111:75–81.
46. **Nakashima AS, Oddo S, Laferla FM, Dyck RH.** Experience-dependent regulation of vesicular zinc in male and female 3xTg-Ad mice. *Neurobiol Aging*. 2010;31:605–613.
47. **Lee JY, Cole TB, Palmiter RD, Suh SW, Koh JY.** Contribution by synaptic zinc to the gender-disparate plaque formation in human Swedish mutant APP transgenic mice. *Proc Natl Acad Sci USA*. 2002;99:7705–7710.
48. **Beltramini M, Zambenedetti P, Wittkowski W, Zatta P.** Effects of steroid hormones on the Zn, Cu and MTI/II levels in the mouse brain. *Brain Res*. 2004;1013:134–141.
49. **Song MK, Kim YY, Heng MCY, Adham NF, Ament ME.** Prostaglandin interacts with steroid sex hormones in the regulation of intestinal zinc transport. *Comp Biochem Physiol*. 1992;101A:477–481.
50. **Costello LC, Liu Y, Zou J, Franklin RB.** Evidence for a zinc uptake transporter in human prostate cancer cells which is regulated by prolactin and testosterone. *J Biol Chem*. 1999;274:17499–17504.
51. **Taylor KM, Morgan HE, Smart K, et al.** The emerging role of the LIV-1 subfamily of zinc transporters in breast cancer. *Mol Med*. 2007;13:396–406.
52. **Ola MS, Nawaz M, Ahsan H.** Role of Bcl-2 family proteins and caspases in the regulation of apoptosis. *Mol Cell Biochem*. 2011; 351:41–58.
53. **Pietsch EC, Sykes SM, McMahon SB, Murphy ME.** The p53 family and programmed cell death. *Oncogene*. 2008;27:6507–6521.
54. **Sinha K, Das J, Pal PB, Sil PC.** Oxidative stress: the mitochondria-dependent and mitochondria-independent pathways of apoptosis. *Arch Toxicol*. 2013;87:1157–1180.
55. **Feng P, Li TL, Guan ZX, Franklin RB, Costello LC.** Direct effect of zinc on mitochondrial apoptogenesis in prostate cells. *Prostate*. 2002;52:311–318.
56. **Feng P, Li T, Guan Z, Franklin RB, Costello LC.** The involvement of Bax in zinc-induced mitochondrial apoptogenesis in malignant prostate cells. *Mol Cancer*. 2008;7:25.
57. **Papadopoulou N, Charalampopoulos I, Anagnostopoulou V, et al.** Membrane androgen receptor activation triggers down-regulation of PI-3K/Akt/ NF-κB activity and induces apopototic responses via Bad, FasL and caspase -3 in DUI145 prostate cancer cells. *Mol Cancer*. 2008;7:88.
58. **Kampa M, Nifli AP, Charalampopoulos I, et al.** Opposing effects of estradiol- and testosterone-membrane binding sites on T47D breast cancer cell apoptosis. *Exp Cell Res*. 2005;307:41–51.
59. **Uhlén M, Björling E, Agaton C, et al.** A human protein atlas for normal and cancer tissues based on antibody proteomics. *Mol Cell Proteomics*. 2005;4:1920–1932.
60. **Franz M-C, Anderle P, Bürzle M, Suzuki Y, et al.** Zinc transporters in prostate cancer. *Mol Aps Med*. 2013;34:735–741.
61. **Grattan BJ, Freake HC.** Zinc and cancer: implications for LIV-1 in breast cancer. *Nutrients*. 2012;4:648–675.
62. **Hanby AM.** The pathology of breast cancer and the role of the histopathology laboratory. *Clin Oncol (R Coll Radiol)*. 2005;17: 234–239.
63. **Berges RR, Vukanovic J, Epstein JI, et al.** Implication of cell kinetic changes during the progression of human prostatic cancer. *Clin Canc Res*. 1995;1:473–480.
64. **Berg AH, Rice CD, Rahman Md S, Dong J, Thomas P.** Identification and characterization of membrane androgen receptors in the ZIP9 zinc transporter subfamily: I. Discovery in female Atlantic croaker and evidence ZIP9 mediates testosterone-induced apoptosis of ovarian follicle cells. *Endocrinology*. 2014;155:4237–4249.